

Analysis of GPS-Based Relative Navigation Schemes for Earth Observation Missions Relying on Cooperating Satellites

Alfredo Renga, *University of Naples "Federico II"*
Urbano Tancredi, *University of Naples "Parthenope"*
Michele Grassi, *University of Naples "Federico II"*

BIOGRAPHY

Alfredo Renga received the M.S. degree in aerospace engineering from the University of Naples, Naples, Italy, in 2006. Since November 2006, he is a Ph. D. student at Department of Aerospace Engineering, "Federico II". His current field of research includes Bistatic and Interferometric SAR system for Earth and planetary remote sensing and Precise Relative Navigation of Formation Flying Spacecrafts by GPS.

1 INTRODUCTION

This paper addresses the problem of developing a filtering approach to achieve robust and accurate relative navigation in formation flying. Formation flying is a topic of high interest since there are many examples of space programs based on using co-flying satellites. In such applications the platforms are co-orbiting and fly by maintaining prefixed relative orbital geometries, designed so to achieve specific mission objectives. In many cases multiple platforms act coordinately to synthesize a unique payload. In other cases, the platforms complement to each other so to magnify mission scientific goals or perform specific in-orbit operations as refueling or servicing (as in on-orbit servicing missions).

Space missions based on co-orbiting platforms demand for increasing level of autonomy. Indeed, maintaining specific relative orbital geometries or performing maneuvers as proximity flight or fly around requires tasks as relative navigation and control to be performed with high levels of autonomy and accuracy, and in real-time. To this end technologies based on differential GPS and vision and laser systems have been proposed, with performance depending on implemented techniques and algorithms and on the considered applications.

With regard to GPS-based techniques, in the recent years several approaches and techniques have been investigated and tested, numerically or in ground test beds, to filter out Carrier-phase GPS (CDGPS) measurements to determine accurately the relative positions of formation flying satellites, in real-time or post-processing [1]-[2]. However, these techniques are usually application-based, i.e. they are developed and tuned on specific relative orbit scenarios in which the inter-satellite distance does not experience large variations [1]. Instead, the approach proposed in this paper aims at providing a mean to accurately determine the baseline in missions in which the relative orbit configuration and the inter-satellite distance largely vary due to specific mission requirements [3]-[6]. As an example, remote sensing applications based on bistatic synthetic aperture radar (SAR) require the implementation of different observation geometries, characterized by the inter-satellite distance varying from hundreds meters to hundreds kilometers [4]-[5]. Related scientific goals typically require a baseline determination accuracy ranging from a few millimeters to a few centimeters. In addition, when separation between satellites is short, such accurate baseline determination must be performed in real-time for formation flying control and collision avoidance maneuvers. This requires both using dual-frequency GPS receivers and implementing filtering techniques capable of providing accuracy and robustness in the relative navigation.

In this paper performance of Carrier-phase Differential GPS (CDGPS) for relative navigation in applications where the inter-satellite distance highly varies along the orbit is investigated. Specifically, to satisfy high accuracy requirements, a hybrid filtering approach is proposed in which a dynamic filter is combined in cascade with a kinematic one. For the dynamic filter both an Extended Kalman Filter (EKF) and an Unscented Kalman Filter (UKF)

are evaluated and compared to output high-accuracy estimates of the floating values of the carrier-phase integer ambiguities. These, once extracted with the LAMBDA method, are processed in the kinematic filter to come to highly precise relative position and velocity estimates. To achieve real-time application the filter state dimension has to be limited as much as possible. In addition, the relative dynamics model has to be maintained as simple as possible. To this end, an approach processing double-difference carrier phase observables has been followed and a Keplerian dynamics model has been used for the time-update stage of the dynamic filter. In order to achieve high accuracy estimates of the integer ambiguity floating values ionosphere delays terms shall be included in the filter state, especially in long-baseline applications. In using double difference measurement equations, these delay terms are very small but still enough large if sub-centimeter to centimeter level accuracy is desired. Thus, in order to improve their estimate an original approach is followed in which they are expressed in terms of the Vertical Total Electron Content (VTEC) that is introduced in the filter state. As it will be shown in the paper, this allows improving filter performance, especially in long-baseline applications, with respect to estimating directly double-difference ionosphere delay terms. Filter approach performance is preliminarily evaluated by numerical simulations of relevant orbital scenarios.

2 FILTER MODEL

Real-time relative navigation of formation-flying satellites requires the implementation of a dynamic filtering scheme relying on a non-linear model of the satellites' relative dynamics. In addition, typical bias terms of GPS observables, such as carrier phase ambiguities and ionosphere path delays, must be taken into account during the filtering process in order to improve filter robustness and accuracy.

The filter model has been developed with reference to the Earth-Centered-Earth-Fixed (ECEF) reference frame and a formation of two satellites, named master (#1) and slave (#2), (see Fig. 1). The relative navigation problem is well described by the following nonlinear discrete stochastic model with additive white noise

$$\begin{cases} x(n+1) = g_n[x(n), v_n] \\ y(n) = h_n[x(n), w_n] \end{cases} \quad (1)$$

x is the system state vector, y is the measurement vector, g is the non-linear state propagation function, h is the non-linear observation function, w is the process noise vector, v is measurement noise

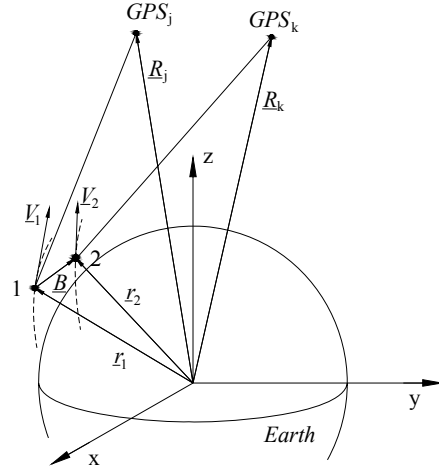


Fig. 1. GPS relative navigation geometry (not to scale for clarity)

vector, which are assumed to be Gaussian and mutually independent, and n stands for the time epoch t_n . Covariance matrixes are also introduced for the variables defined in Eq.(1), as: P_{xx} for x , P_{yy} for y , Q for v and R for w . The measurement model relies on dual-frequency, double difference (DD) observables. The state and the measurement vectors are thus given as

$$x = \begin{bmatrix} B \\ \dot{B} \\ VTEC_1 \\ VTEC_2 \\ L_1 AM \\ L_2 AM \end{bmatrix}_{8+2(N_{sat}-1)} ; y = \begin{bmatrix} L_1 PR \\ L_2 PR \\ L_1 CP \\ L_2 CP \end{bmatrix}_{4(N_{sat}-1)} \quad (2)$$

where N_{sat} is the number of commonly viewed GPS satellites, $VTEC_1$ and $VTEC_2$ are the vertical total electron content from, respectively, the master and slave receiver to the upper bound of the ionosphere, $L_1 AM$ and $L_2 AM$ are the DD integer ambiguity vectors, respectively, on L1 and L2 carriers, $L_1 PR$ and $L_2 PR$ are the pseudorange vectors, and $L_1 CP$ and $L_2 CP$ are the carrier phase vectors.

Fig. 2 shows a conceptual representation of the filtering scheme [7]. At the generic time step n the filter receives in input the estimates of the state vector and the covariance matrix, P_{xx} , at the previous step, along with the GPS observables from master and slave satellites, respectively. A coarse evaluation of the master satellite ECEF position must be provided as well. Measurements from commonly available GPS satellites are extracted in order to calculate DD observables. Since both the number of commonly viewed GPS satellite and the pivot satellite can change between subsequent observations a rearranging/re-initialization step is

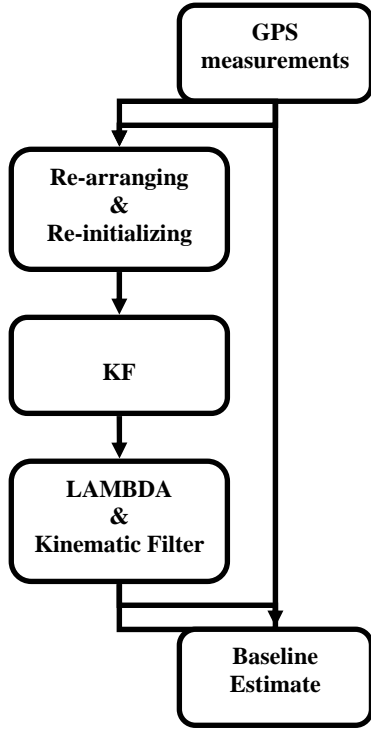


Fig. 2. Block diagram of the filtering scheme [7].

needed to correctly relate the bias term of the state vector to the current measurements. In more details, a variation of the pivot satellite implies a complete re-initialization of all the terms depending on VTEC and carrier phase ambiguities either for the state vector or for the state covariance matrix. This is one major reason why usually DD-based dynamic filters are not used. On the contrary, new/disappeared GPS satellites impact only isolated bias terms, which must be reinitialized or removed. A specific procedure has been developed to effectively manage pivot and satellite number variations in order to ensure filter convergence [8]. It is worth outlining that this procedure is a major step in the filtering scheme, since it strongly affects performance. The rearranged state vector and covariance matrix are used as inputs to a Kalman Filter (KF). Two different Kalman Filtering strategies are considered, namely the Extended Kalman Filter (EKF) and the Unscented Kalman Filter (UKF). The next section reports a detailed description of both EKF and UKF. The purpose of using a KF is performing a robust floating estimate of the DD ambiguities, whose integer values are then extracted by using a least square integer search algorithm (the LAMBDA method [9],[10] is used in this study). This allows correcting the individual DD carrier phase observations, which can be then used within a kinematic approach based on a Weighted Least Square (WLSQ) algorithm to produce a highly accurate baseline estimation. Residual errors in the carrier phase observables depend mainly on DD

ionosphere path delays estimation errors. A common procedure to eliminate this effect is evaluating ionosphere free combinations of corrected carrier phase observables, as in [8], [2].

For completeness it is important to remark that an estimate of the master satellite ECEF position is needed for filter implementation. In order to reduce the computational load, a simple WLSQ algorithm based on ionosphere free combinations of the master satellite's pseudorange observables is used to estimate master satellite ECEF position at each time step. This leads to estimation errors ranging from several meters to tens of meters especially if the Geometric Dilution of Precision (GDOP) is poor. Anyway, as it will be shown in the next sections, this coarse master position estimate does not prevent a precise relative navigation with the proposed filtering scheme.

2.1 DYNAMIC MODEL AND STATE PROPAGATION

Non-linear Keplerian equations have been selected for modeling satellites' relative motion in ECEF

$$\begin{aligned}
 \ddot{\underline{B}}_x &= \frac{\mu}{r_1^3} \left[r_{1x} - \frac{r_1^3 (r_{1x} + B_{1x})}{\sqrt{(r_1^2 + B^2 + 2\underline{r}_1 \cdot \underline{B})^3}} \right] + \\
 &\quad \Omega_E^2 B_x + 2\Omega_E \dot{B}_y + w_{\ddot{B}_x} \\
 \ddot{\underline{B}}_y &= \frac{\mu}{r_1^3} \left[r_{1y} - \frac{r_1^3 (r_{1y} + B_{1y})}{\sqrt{(r_1^2 + B^2 + 2\underline{r}_1 \cdot \underline{B})^3}} \right] + \\
 &\quad \Omega_E^2 B_y - 2\Omega_E \dot{B}_x + w_{\ddot{B}_y} \\
 \ddot{\underline{B}}_z &= \frac{\mu}{r_1^3} \left[r_{1z} - \frac{r_1^3 (r_{1z} + B_{1z})}{\sqrt{(r_1^2 + B^2 + 2\underline{r}_1 \cdot \underline{B})^3}} \right] + \\
 &\quad w_{\ddot{B}_z}
 \end{aligned} \tag{3}$$

In Eq.(3), \underline{r}_1 is the master satellite position vector, μ is Earth gravitational parameter, and Ω_E is the Earth angular velocity. The choice of a Keplerian dynamics has to be interpreted as a trade-off between using a nonlinear model to improve accuracy and having a computational load adequate to real-time implementation. \underline{B} and $\dot{\underline{B}}$ are then propagated using a 4th order Runge-Kutta integration method. The remaining state vector components are treated as random walk plus random constant processes [11].

2.2 OBSERVATION EQUATIONS

The measurement model is based on DD observables. A double difference can be formed by subtracting two single difference equations of the same type and frequency, taken by the same two GPS receivers at the same time from two different GPS satellites, one of which, named pivot and denoted as j , is taken as a reference (see Fig. 1). The pivot satellite is selected as the one with the highest elevation with respect to the master. On this basis, the dual-frequency DD observation model is given as

$$\begin{aligned} L_1 PR_{12}^{jk} &= \rho_{12}^{jk} + \\ &\quad \left(L_1 J_2^{jk} VTEC_2 - L_1 J_2^{jk} VTEC_1 \right) + PR_{L_1} v_{12}^{jk} \\ L_2 PR_{12}^{jk} &= \rho_{12}^{jk} + \\ &\quad \frac{f_{L_1}^2}{f_{L_2}^2} \left(L_2 J_2^{jk} VTEC_2 - L_2 J_2^{jk} VTEC_1 \right) + PR_{L_2} v_{12}^{jk} \quad (4) \\ L_1 CP_{12}^{jk} &= \rho_{12}^{jk} - \left(L_1 J_2^{jk} VTEC_2 - L_1 J_2^{jk} VTEC_1 \right) + \\ &\quad \lambda_{L_1 L_1} AM_{12}^{jk} + CP_{L_1} v_{12}^{jk} \\ L_2 CP_{12}^{jk} &= \rho_{12}^{jk} - \frac{f_{L_1}^2}{f_{L_2}^2} \left(L_2 J_2^{jk} VTEC_2 - L_2 J_2^{jk} VTEC_1 \right) + \\ &\quad \lambda_{L_2 L_2} AM_{12}^{jk} + PR_{L_2} v_{12}^{jk} \end{aligned}$$

where f is the GPS signal frequency, λ is the GPS signal wavelength, k indicates the generic GPS satellite, and

$$\rho_{12}^{jk} = \left\| \underline{R}_k - (\underline{r}_1 + \underline{B}) \right\| - \left\| \underline{R}_k - \underline{r}_1 \right\| - \left\| \underline{R}_j - (\underline{r}_1 + \underline{B}) \right\| + \left\| \underline{R}_j - \underline{r}_1 \right\| \quad (5)$$

is the DD signal path. Ionospheric path delays are related to $VTEC$ by the well-known mapping formula [12]

$$L_1 J_1^{jk} = L_1 J_1^k - L_1 J_1^j \quad (6)$$

$$L_1 J_i^k = \frac{82.1}{f_{L_1}^2 \left(\sqrt{\sin^2 \gamma_{ik} + 0.076} + \sin \gamma_{ik} \right)} \quad (7)$$

where γ_{ik} is the elevation on the horizon of GPS satellite k , as measured by the receiver i .

2.3 KALMAN FILTER EQUATIONS

Within the filtering scheme of Fig. 2, the KF block is in charge of providing a first estimate of the baseline components, of the ionospheric delays (in terms of VTEC for the two satellites) and of the float DD ambiguities for the subsequent integer ambiguities resolution. This is done by applying KF estimation theory to the nonlinear dynamical system defined by Eq.(3) augmented with random walk processes for modeling float ambiguities and VTEC terms, and by employing the observation model of section 2.2.

As previously discussed, two different Kalman Filtering strategies are applied herein, namely the EKF and the UKF. The estimate update equations are common to both Kalman filtering schemes. Using the notation $\Pi(i | j)$ to be the variable Π at time i conditioned on all measurement up to time j , the well-known KF estimate update equations, in the more general form, are given by:

$$\hat{x}(n|n) = \hat{x}(n|n-1) + K_n z_n \quad (8)$$

$$P_{xx}(n|n) = P_{xx}(n|n-1) - K_n P_{zz}(n|n-1) K_n^T \quad (9)$$

where \hat{x} stands for the estimated value of x , \hat{y} is the expected measurement, and $z_n = y_n - \hat{y}_n$ is the innovation vector, that is, the difference between the actual and the expected measurement, and its covariance is denoted as P_{zz} . The Kalman gain at time n , K_n , is given by:

$$K_n = P_{xy}(n|n-1) P_{zz}^{-1}(n|n-1) \quad (10)$$

2.3.1 Extended Kalman Filter

The EKF builds upon linearization of the observation model and of the nonlinear system at the current best estimate of the state vector. The predicted state and state covariance thus are:

$$\hat{x}(n|n-1) = g_{n-1} \left[\hat{x}(n-1|n-1), 0 \right]$$

$$P_{xx}(n|n-1) = \Phi_n P_{xx}(n-1|n-1) \Phi_n^T + Q_n \quad (11)$$

and the measurement equations are given by:

$$\hat{y}_n = h_n \left[\hat{x}(n|n-1), 0 \right]$$

$$P_{zz}(n|n-1) = H_n P_{xx}(n|n-1) H_n^T + R_n \quad (12)$$

where Φ_n and H_n are the Jacobians of the $g_n(\cdot)$ and $h_n(\cdot)$ functions, evaluated on the best available estimate of the state vector. We wish to emphasize that, thanks to the relatively simple analytical model proposed in Eq.(3) for describing the relative dynamics of the two satellites, explicit analytical expression can be employed for both Φ_n and H_n , thus avoiding the need for numerical computations of the Jacobians. Taking advantage of the prediction and measurement equations of the EKF, the estimate update equations (8) – (9) specialize to:

$$\hat{x}(n|n) = \hat{x}(n|n-1) + K_n z_n$$

$$P_{xx}(n|n) =$$

$$(I - K_n H_n) \left[P_{xx}(n|n-1) \right] (I - K_n H_n)^T + K_n R_n K_n^T$$

$$K_n = P_{xx}(n|n-1) H_n^T \left[H_n P_{xx}(n|n-1) H_n^T + R_n \right]^{-1} \quad (13)$$

2.3.2 Unscented Kalman Filter

The UKF makes use of the Unscented Transformation (UT) for predicting the mean and covariance of the state vector x at time n , given its mean and covariance at time $n-1$. The UT, first introduced in [13], basically allows to estimate the mean and covariance of a nonlinear function by computing the mean and covariance of the discrete set of points obtained by propagating a set of deterministically chosen points through the nonlinear function itself. The points to propagate, usually denoted as “sigma points”, are chosen based on the mean and variance of the independent variable.

Compared to conventional linearization and propagation of the state vector’s statistics, the UT has the advantage of providing unbiased estimates with a higher accuracy of both mean and covariance (see [14] for a detailed discussion of the UT approximation capabilities). Several forms of the UT have been proposed after the standard one was published. Within Kalman Filtering applications, the Scaled Unscented Transformation (SUT) (ref. [15]) is the most applied, and it is employed in the present context as well. It requires numerical propagation of the state vector at each step of the KF to be carried out $2N_x + 1$ times, where N_x stands for the dimension of the state vector.

Application of the SUT in Kalman filtering schemes can be carried out in different ways, depending on how the process and measurements noises are treated. More precisely, since the UT can handle nonlinear processes and noises, there is the possibility of augmenting the process state vector with process and observation noises, in order to take into account also noise effects in computing the mean [13]. Nonetheless, when process and measurement noise are purely additive, the computational complexity of the UKF can be reduced by avoiding to augment the state vector with the noise random variables [16]. This significantly reduces the number of numerical propagations needed at each filter cycle, with corresponding computational benefits, even though the resulting filter does not take into account nonlinear effects of the process noise on the state estimate. Since the application we present is aimed at real-time relative navigation, limiting the computational load required for positioning is of great importance. For this reason, and because the process and observation noises we refer to are purely additive, we employ a non-augmented UKF.

In order to apply the update equations (8) – (9), the UKF algorithm has to predict the relevant

variables. In order to predict the new state and covariance at time n , the SUT is applied to $2N_x + 1$ sigma points drawn from $\hat{x}(n-1|n-1)$. The SUT application consists in performing the following steps:

1) Compute the set of sigma points and associated weights from the $N_x \times N_x$ matrix $P_{xx}(n-1|n-1)$. Using the SUT this step is done as follows, where $\lambda := \alpha^2(N_x + \kappa) - N_x$:

$$\begin{aligned} X_0 &= \hat{x}(n-1|n-1) \\ X_i &= \hat{x}(n-1|n-1) + \\ &\quad \left[\sqrt{[N_x + \lambda] P_{xx}(n-1|n-1)} \right]_i \quad i = 1, \dots, N_x \\ X_i &= \hat{x}(n-1|n-1) - \\ &\quad \left[\sqrt{[N_x + \lambda] P_{xx}(n-1|n-1)} \right]_{i-N_x} \quad i = N_x + 1, \dots, 2N_x \\ W_0^{(m)} &= \frac{\lambda}{N_x + \lambda} \\ W_0^{(c)} &= W_0^{(m)} + (1 - \alpha^2 + \beta) \\ W_i^{(m)} &= W_i^{(c)} = \frac{1}{2(N_x + \lambda)} \quad i = 1, \dots, 2N_x \end{aligned} \quad (14)$$

2) Propagate each of the $2N_x + 1$ sigma points through the nonlinear dynamical function $g_{n-1}(\cdot)$ to obtain a *transformed* set of sigma points:

$$X_i(n|n-1) = g_{n-1}[X_i(n-1|n-1), 0] \quad (15)$$

3) Compute the predicted mean and covariance with the following equations:

$$\hat{x}(n|n-1) = \sum_{i=0}^{2N_x} W_i^{(m)} X_i(n|n-1) \quad (16)$$

$$\begin{aligned} P_{xx}(n|n-1) &= \sum_{i=0}^{2N_x} \left\{ W_i^{(c)} [X_i(n|n-1) - \hat{x}(n|n-1)] \cdot \right. \\ &\quad \left. [X_i(n|n-1) - \hat{x}(n|n-1)]^T \right\} + Q_n \end{aligned} \quad (17)$$

In order to determine the equivalent statistics for the innovations sequence one should evaluate the expected measurements taking into account the propagated mean and covariance of the state: $\hat{x}(n|n-1)$, $P_{xx}(n|n-1)$. For doing this using the SUT, one cannot use the propagated sigma points $X_i(n|n-1)$ [17]. Indeed, such points are not consistent with $P_{xx}(n|n-1)$, because of the addition of Q_n to the sigma points’ covariance matrix in Eq.(12). As a consequence, one has to obtain a new set of sigma points $X'_i(n|n-1)$ that are consistent with the propagated mean and covariance of the state vector, that is, that are based on the mean

$\hat{x}(n|n-1)$ and on the covariance matrix $P_{xx}(n|n-1)$. In practice, a *resampling* step is necessary, even though the weights W_i are not affected by this process, and do not need to be re-computed.

The equivalent statistics for the innovations sequence can now be determined by instantiating each new sigma point through the measurement model:

$$Y_i(n|n-1) = h_n [X_i'(n|n-1), 0], \quad i = 0, \dots, 2N_x$$

and computing the expected measurement as:

$$\hat{y}_n = \sum_{i=0}^{2N_x} W_i^{(m)} Y_i(n|n-1) \quad (18)$$

The innovation covariance P_{zz} is given by the sum between the covariance matrices of the measurements and of the measurement noises:

$$P_{zz}(n|n-1) = \sum_{i=0}^{2N_x} \left\{ W_i^{(c)} [Y_i(n|n-1) - \hat{y}_n] \cdot [Y_i(n|n-1) - \hat{y}_n]^T \right\} + R_n \quad (19)$$

At last, noting that the additive disturbances w_n and v_n are uncorrelated, the cross correlation matrix can be determined as above, using the sigma points consistent with the propagated state vector statistics, that is, $X_i'(n|n-1)$:

$$P_{xy}(n|n-1) = \sum_{i=0}^{2N_x} \left\{ W_i^{(c)} [X_i'(n|n-1) - \hat{x}(n|n-1)] \cdot [Y_i(n|n-1) - \hat{y}_n]^T \right\} \quad (20)$$

The complete UKF model is thus obtained substituting Eq.s (16)-(20) into Eq.s (8)-(10), which we omit for brevity.

3 APPLICATION CASE

A filter implementation example is reported in this section. The filter is assumed to provide real-time relative positioning. However, real time implementation issues are not addressed herein. We instead evaluate the overall runtime required by the filter on a standard non-real time computer, in order to address the suitability of a future real-time filter implementation. The master satellite is supposed to receive slave GPS observables by a satellite inter-link; such a link is usually available in formation flying satellites for payload synchronization. All the filtering computations are assumed to be performed by the processing unit onboard the master satellite.

The filter performance is here estimated by comparing the positioning results with the “true

values” generated by the simulation environment. In such a way, the effectiveness of the proposed filtering approach is evaluated, even though on a single, specific, instance of the selected orbital scenario. Time-consuming Monte Carlo validation activities are foreseen in the near future.

Hence, a single-orbit scenario will be considered in the following. As a consequence filter tuning is determined by a constant set of values. As for state vector initialization, the baseline and relative velocity initial values are evaluated by differencing the position and velocity vector of the master and slave satellite. These are estimated by an iterative WLSQ algorithm applied to pseudorange and Doppler observables, respectively. *VTEC* is initialized at a mean orbital value and the initial DD integer ambiguities are evaluated from DD pseudo path length [8].

3.1 SIMULATION ENVIRONMENT

Filter performance is numerically evaluated by using the Satellite Navigation Toolbox 3.0 for Matlab[®] developed by GPSofT, Inc. [18]. The toolbox allows simulating the GPS satellite constellation, the propagation environment and the receiver measurements.

Filter performance is evaluated with reference to two different satellite orbital scenarios. To specifically evaluate filter performance in missions with highly variable baselines a satellite formation has been considered based on parallel or pendulum orbits, which share eccentricity, inclination, semi-major axis and anomaly of perigee [19]. In the considered formation, whose orbital parameters are reported in *Table 1*, the baseline attains a maximum value of 200 km at the equator, and a minimum value of a few kilometers at the highest latitudes. This orbital design reflects next generation monostatic/bistatic spaceborne SAR mission needs in LEO [20], where the Italian COSMOSkyMed mission [21] has been considered as a reference for the orbit of the monostatic sensor. An additional orbital scenario is considered, based on leader-follower formations characterized by a constant baseline of 200 km (see *Table 1*). Filter performance is evaluated by comparison with reference orbits obtained with an orbit propagator including a seven-order model of the gravitational field and the aerodynamic drag.

The Satellite Navigation Toolbox was developed mainly for Earth-based GPS receiver, so in order to use it for satellites in LEO an important modification to the ionosphere delay model is introduced. Satellite Navigation Toolbox has been

Table 1. Orbital parameters of master and slave satellites

	Master	Slave	
		Pendulum 200 km	Lead.-Foll. 200 km
Semi-major axis (km)	6997.94	6997.94	6997.94
Eccentricity	0.00118	0.00118	0.00118
Anomaly of perigee (°)	90	90	90
Inclination (°)	97.87	97.87	97.87
Ascending node right ascension (°)	0	1.680	0
Initial mean anomaly (°)	0	0.3406	1.6376
Ballistic coefficient (kg/m ²)	113.33	106.25	106.25

completed by first [12] and second order [22]-[23] ionosphere delay models. Moreover the actual status of Earth ionosphere has been simulated by implementing the International Reference Ionosphere [24].

In the simulations, the LAGRANGE receiver nominal performances are used as reference [25]. It is an integrated GPS receiver for spaceborne applications, characterized by 12 dual-frequency channels and 0.5-m and 1.2-mm representative measurement uncertainty, for code and carrier phase, respectively; 1-Hz GPS data frequency update is considered.

3.2 SIMULATION RESULTS

The insertion of VTEC in the state vector represents an important change compared with classic EKF schemes for relative navigation of formation-flying satellites by GPS, which usually consider ionosphere path delay terms modeled as random walk processes [2]. Actually, ionosphere path delays are time-variable and their variation has a twofold origin. Indeed, from one observation to the subsequent, VTEC changes, but relative geometry among master, slave, pivot, and generic GPS satellite changes too, thus generating a variation of GPS satellites' elevations with respect to master and slave receivers, and therefore different values result from the mapping formula. The use of VTEC in state vector can be interpreted as a way to isolate the second source of variation thanks to the approximate knowledge of, respectively, master satellite position, baseline, and GPS satellites' position.

Classical approaches provide good results only if very accurate relative dynamic models are available,

and so, only for post-processing implementations. In such a case high enough ionosphere process noise must be added at every time to guarantee a proper ambiguity resolution [2]. However when dealing with real-time estimation problem the relative dynamic is less accurate and therefore high ionosphere process noise leads to incorrectly resolved integer ambiguities with associated local spikes or divergences of the baseline estimation error [8].

Fig. 3 shows a comparison between DD ionosphere terms evaluated by the filter proposed in this paper and a filter including DD ionosphere terms in the state vector [7]-[8]. It is immediate to note that the VTEC model allows following the true variation of DD ionosphere terms, whereas the simple modeling of DD ionosphere terms as random walk produces estimation errors of the same order of magnitude of true ionosphere terms. Moreover, when DD ionosphere terms are inserted in the state vector a change in the pivot satellite forces the filter to re-initialize (i.e. to set to zero) the whole vector of estimated ionosphere delays (see Fig. 4). On the other hand, the VTEC is not affected at all by pivot variations, and the ionosphere delays change only to reflect the different elevation angles to consider in Eqs. (6), (7).

The comparison between the true baseline vector of the leader-follower formation of Table 1 and the baseline components estimated by the EKF and the UKF strengthens this last statement (see Fig. 5 and Fig. 6). The insertion of VTEC in the state vector yields an increase of the filter robustness with respect to the solution proposed in [7]-[8]: DD integer ambiguities are always estimated correctly and so the baseline estimation error has a uniform behavior along the orbit. The only exception is a short orbital arc where the number of commonly observed GPS satellite drops to 4: in such a case only three DD iono-free corrected carrier phase observables are available for calculating the baseline components. Along track (and cross-track too, not reported for brevity) error is characterized by a mean of -3.96 mm of and a standard deviation of 11.7 mm whereas the radial error is generally higher, with a mean error of 0.48 mm and a standard deviation of 32.2 mm, as common in GPS navigation [26].

Finally it is important to remark that EKF and UKF seem to achieve very similar performance. This is not an unexpected result if we consider that once the integer ambiguities have been correctly calculated, the two filtering approaches apply the same kinematic algorithm to the same corrected

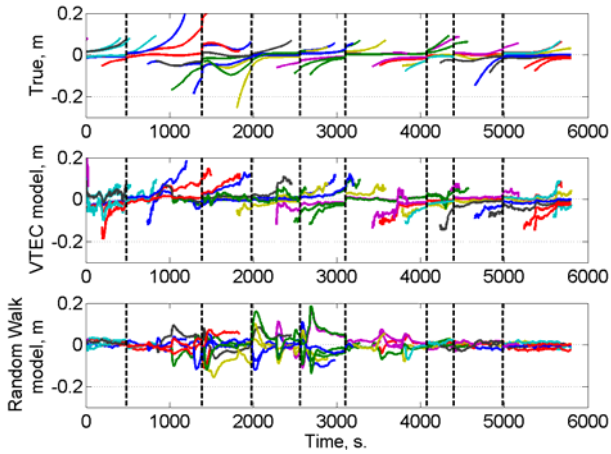


Fig. 3. True vs. estimated ionospheric delays in one orbit (dashed vertical lines at pivot change events)

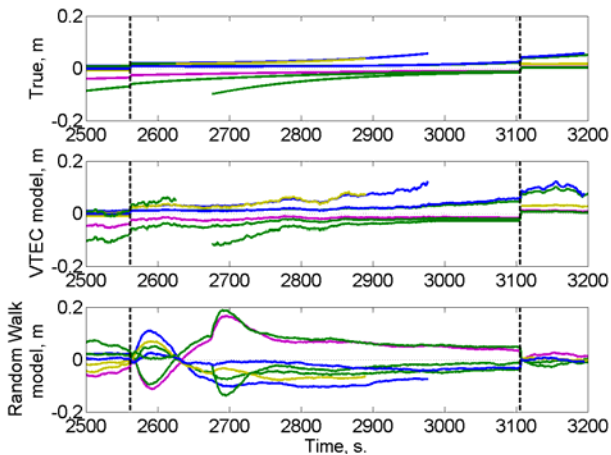


Fig. 4. Pivot change effects on true vs. estimated ionospheric delays

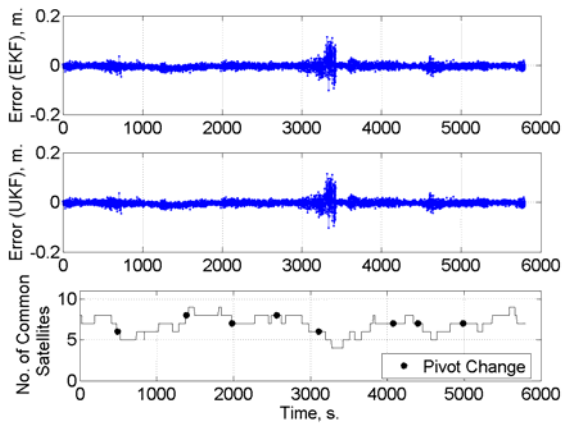


Fig. 5. Along track baseline estimation error; Leader – Follower orbit.

ionosphere-free carrier phase measurements. Therefore, once a filter model has been set that allows estimating the floating values of the integer ambiguities with adequate accuracy so that corresponding integer values can be uniquely identified with the LAMBDA method, there is no advantage in using a nonlinear filter with respect to

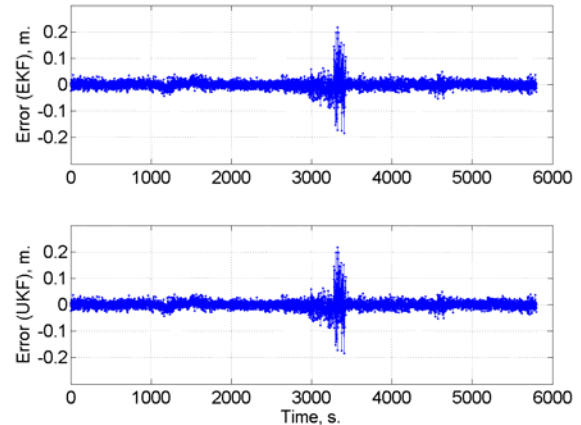


Fig. 6. Radial baseline estimation error; Leader – Follower orbit.

a classical EKF. Of course this results should be validated by further analyses.

Very high baseline variations (Fig. 7) can be critical for satellite relative navigation. EKF with DD ionosphere terms within the state vector ([7]-[8], [2]) showed performance variable with the baseline [8]. The separation between the two variation sources of ionosphere path delay terms operated by the proposed filter allows avoiding this limitation. As a consequence, the estimation error is not affected by the actual baseline length and it exhibits an uniform behavior along the orbit (see Fig. 8 – Fig. 10), with the only exception of the short orbital path characterized by a low number of commonly viewed GPS satellites. Performance is close to the one estimated for the leader-follower formation, i.e. for constant baseline: mean cross-track estimation error of 0.7 mm with a standard deviation of 9 mm, whilst a larger radial estimation error with 0.8 mm mean error and 31.2 mm standard deviation is achieved.

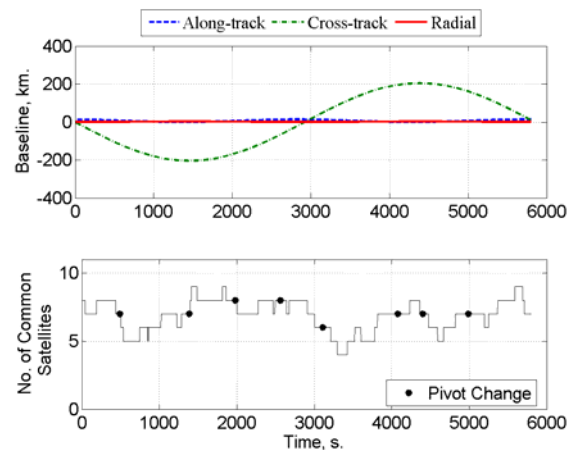


Fig. 7. True baseline time history and GPS satellites visibility; Pendulum orbit.

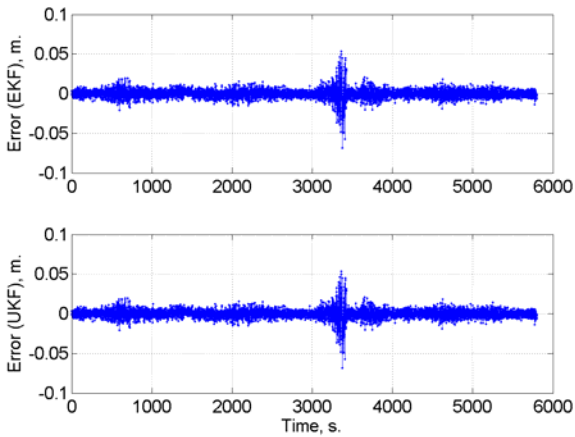


Fig. 8. Along track baseline estimation error; Pendulum orbit.

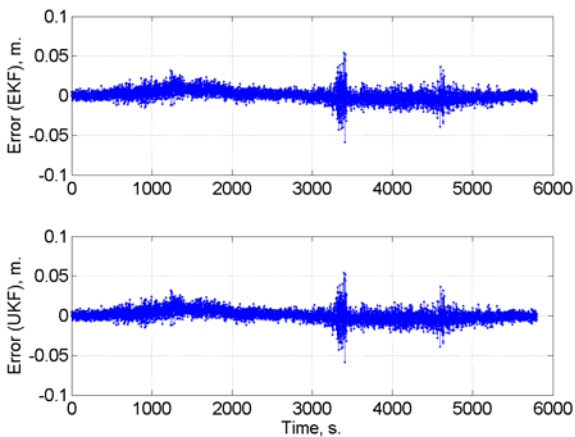


Fig. 9. Cross track baseline estimation error; Pendulum orbit.

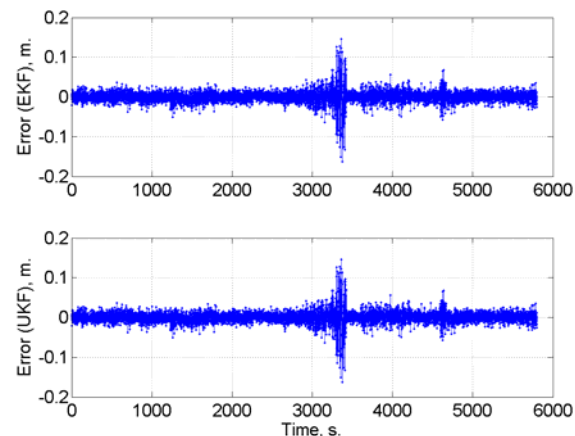


Fig. 10. Radial baseline estimation error; Pendulum orbit.

Concerning the computational load requested by the filter, a preliminary evaluation suggests that both the EKF-based scheme and the UKF one have the potentials for providing real-time relative positioning at 1 Hz. Indeed, numerical simulation of both orbital scenarios in Matlab[®] were obtained in ~ 4 and ~ 27 minutes (in face of a simulated time span of ~ 96 minutes) for the EKF and the UKF,

respectively, using a standard desktop PC equipped with a Pentium IV 2.4 GHz processor and 2GB RAM.

4 CONCLUSIONS

A hybrid filtering scheme has been described in the paper that allows estimating the baseline between formation flying satellites with high accuracy and in real-time. The proposed scheme combines the robustness of a dynamic filter, that processes double-difference observables, and the accuracy of a kinematic one, that processes ionosphere-free double-difference combinations. In addition, since space applications in which large values of the baseline are achieved are considered, for the dynamic filter both an Extended Kalman Filter and an Unscented Kalman Filter have been evaluated and performance compared. To achieve high accuracy in baseline estimate an original approach has been developed in which the dynamic filter state is augmented with the Vertical Total Electron Content instead of using ionosphere delay terms modeled as random walk processes.

Filter performance has been evaluated by numerical simulation of relative orbit scenarios relevant to remote sensing applications. Numerical results show that in the proposed approach the two implemented dynamic filters exhibit very similar performance, so no advantages are achieved using a nonlinear filter in long-baseline applications. Instead, computational charge is increased of about 6 times with respect to the one of a classical Extended Kalman Filter, although real-time implementation is possible at 1 Hz updating frequency.

In baseline estimation, the proposed filtering approach allows getting centimeter level performance in real time and for highly varying inter-satellite distances, from a few kilometers to a few hundreds of kilometers.

Results also show that the proposed filtering approach is robust with respect to baseline variation and to sudden changes in the pivot satellite, thanks to an originally developed procedure for filter state re-arrangement and re-initialization, that allows to overcome major limitations in using double-difference dynamic filters.

ACKNOWLEDGEMENTS

This work has been carried out with the financial contribution of the Italian Space Agency and the Ministry of University and Scientific Research.

REFERENCES

- [1] R. Kroes, O. Montenbruck, W. Bertiger, P.N.A.M. Visser, Precise GRACE baseline determination using GPS, *GPS Solutions*, 9(1), 21–31, 2005.
- [2] Kroes R., Precise relative positioning of formation flying spacecraft using GPS, Ph.D Thesis, *Publications on Geodesy* 61, Delft, 2006.
- [3] F. Caltagirone, et al., SABRINA the Italian Mission for Endowing COSMO-SkyMed with Bistatic and Interferometric Capabilities, *Proceedings of EUSAR*, 2006.
- [4] G. Krieger, A. Moreira, Spaceborne bi- and multistatic SAR: Potential and challenges, *Proc. Inst. Electr. Eng.-Radar, Sonar Navig.*, 153, 3, 184–198, 2006.
- [5] A. Moccia and M. D’Errico, Bistatic SAR for Earth Observation, in M. Cherniakov, Editor, *Bistatic Radar: Emerging Technology*, John Wiley & Sons Ltd, Chichester, England, 2008.
- [6] G. Krieger, et al., TanDEM-X: A Satellite Formation for High-Resolution SAR Interferometry, *IEEE Trans. on Geoscience and Remote Sensing*, 45, 11, 3317-3341, 2007.
- [7] A. Renga, M. Grassi, A hybrid approach for GPS-based Relative Navigation of Formation Flying Satellites in Remote Sensing Missions, *Aerotecnica Missili e Spazio*, Vol.87-4, 2008, pp. 183-190 ISSN: 0365-7442. [Online] Available: www.aidaa.it/4-2008/paper2.pdf
- [8] A. Renga, M. Grassi, Precise Relative Navigation for Highly Variable Baselines using carrier-based differential GPS, *59th International Astronautical Congress* Glasgow, Scotland, October 2008. (DVD ISSN 1995-6258,2008, IAC-08 –C1.6)
- [9] Teunissen, P.J.G. , The least-squares ambiguity decorrelation adjustment: a method for fast GPS integer ambiguity estimation, *Journal of Geodesy*, Vol. 70,65-82, 1995.
- [10] de Jonge P., Tiberius C., The LAMBDA method for integer ambiguity estimation: implementation aspects, *LGR-Series Publications of the Delft Geodetic Computing Centre No. 12*, 1996.
- [11] Farrel J., Barth M., The Global Positioning System and Inertial Navigation, *McGraw-Hill*, New York, 1999.
- [12] Montenbruck O., Garcia-Fernandez M., Ionospheric Path Delay Models for Spaceborne GPS, DLR-GSOC TN 05-07; 2005.
- [13] Julier, S., and Uhlmann, J. K., “A general method for approximating nonlinear transformations of probability distributions,” Robotics Research Group, Department of Engineering Science, University of Oxford, Tech. Rep., 1996.
- [14] Julier, S.J.; Uhlmann, J.K., "Unscented filtering and nonlinear estimation," *Proceedings of the IEEE* , vol.92, no.3, pp. 401-422, Mar 2004.
- [15] Julier, S.J., "The scaled unscented transformation," *Proceedings of the 2002 American Control Conference*, vol.6, no., pp. 4555-4559, 2002.
- [16] R. van der Merwe, N. de Freitas, A. Doucet, E. Wan, The unscented particle filter, Technical Report CUED/F-INFENG/TR380, Engineering Department, Cambridge University, August 2000.
- [17] Yuanxin W., Dewen H., Meiping W., Xiaoping H., "Unscented Kalman filtering for additive noise case: augmented versus nonaugmented," *Signal Processing Letters*, IEEE , vol.12, no.5, pp. 357-360, May 2005
- [18] <http://www.gpssoftnav.com/satnav.html>
- [19] M. D’Errico, and A. Moccia, The BISSAT mission: a bistatic SAR operating in formation with COSMO/SkyMed X-band radar, *Aerospace Conf. Proceedings*, IEEE, vol. 2, pp. 2/809-2/818, March 2002.
- [20] A. Renga, A. Moccia, M. D’Errico, et al., From the expected Scientific Applications to the Functional Specifications, Products and Performance of the SABRINA mission, *IEEE Radar Conference*, May 26-30, 2008, Rome, Italy, pp. 1117-1122, IEEE Catalog No. 08CH37940C, ISBN 1-4244-1539-X, ISSN 1097-5659.
- [21] <http://www.cosmo-skymed-ao.asi.it>.
- [22] Mannucchi A. et al., A global mapping technique for GPS-derived ionospheric total electron content measurements, *Radio Science*, Vol. 39, , 1S10,10.1029/2002RS002846A.
- [23] Munake H., A semi-analytical estimation of the effect of second-order ionospheric correction on the GPS positioning, *International Geophys. J.*, 2005, 163, 10-17
- [24] nssdc.gsfc.nasa.gov/space/model/models/iri.html
- [25] LAGRANGE GPS receiver, Thales Alenia Space private communication.
- [26] D. Y. Hsu, Relations between dilutions of precision and volume of tetrahedron formed by four satellites *1994 IEEE Position Location and Navigation Symposium*, pp. 669-676, Apr. 1994.